

Microscopic electro-optical atom trap on an evanescent-wave mirror

A. Shevchenko^{1,a}, T. Lindvall², I. Tuttonen², and M. Kaivola¹

¹ Department of Engineering Physics and Mathematics, Helsinki University of Technology, P.O. Box 2200, 02015 HUT, Finland

² Metrology Research Institute, Helsinki University of Technology, P.O. Box 3000, 02015 HUT, Finland

Received 18 March 2003 / Received in final form 16 October 2003

Published online 9 December 2003 – © EDP Sciences, Società Italiana di Fisica, Springer-Verlag 2003

Abstract. We put forward the idea of a surface-mounted microscopic electro-optical atom trap. The trap is formed on an evanescent-wave atom mirror by the strongly localized static electric field of two oppositely charged transparent electrodes placed close to each other. The electrodes are embedded in a refractive-index-matched thin dielectric layer on the surface of a glass prism. In our example, the phase-space density in the trap center reaches 0.1, when the trap is loaded with atoms from a gravito-optical surface trap.

PACS. 32.80.Pj Optical cooling of atoms; trapping – 39.25.+k Atom manipulation (scanning probe microscopy, laser cooling, etc.)

Much of the recent interest in surface-mounted microscopic atom traps stems from the fact that such traps provide tight confinement for the atoms and thus allow high phase-space densities to be reached. This is attractive in creating quantum-degenerate gases or Bose-Einstein condensates. A few groups have already demonstrated Bose-condensing of Rb atoms in a microscopic magnetic trap [1,2]. All-optical and static-electric field microtraps formed on a planar material surface have also been proposed and some of them have been demonstrated [3–12]. Recently, an all-optical surface-mounted microtrap was used to obtain two-dimensional BEC of Cs atoms [7]. One of the most exciting perspectives in the miniaturization of atom traps lies in realizing integrated atom-optical devices which could make use of the quantum features of coherent matter in quantum information processing. Other possible applications of the microtraps may be found in atom lithography, microscopic acceleration sensing, and in such fundamental studies as investigations of the near-field properties of material surfaces. The possibility to make a trap to have a particularly small size in one or two dimensions opens up an access to experimental studies of dilute atomic gases in restricted geometries.

In this work, we introduce a novel technique to create a microscopic electro-optical atom trap on an evanescent-wave atom mirror. The non-magnetic character of the confining potentials makes the trap free of spin-flip loss [13,14] and, what is more appealing, allows storing of atoms polarized in an arbitrary magnetic quantum state. Then also the lowest state in energy, which is the most stable one against depolarizing collisions [15,16], becomes

available for trapping atoms in. This is not possible for magnetic traps. Furthermore, magnetic tuning of the collisional properties of the atoms [16] becomes possible without perturbing the confining potential. By using the proposed trapping technique one can realize a micrometer-sized 3D atom trap or an atom guide which confines the atoms locally in two dimensions. The latter may have a non-trivial on-plane geometry.

The trap set-up is shown schematically in Figure 1. A thin transparent film is deposited on the upper surface of a glass prism. The film, which has constant thickness, consists of regions of two different materials. One of them is conductive, e.g., indium tin oxide (ITO), and the other one is dielectric. The materials are chosen to have equal indices of refraction at the desired optical wavelength. The conductive part of the film is made in the form of a narrow strip divided in half by a stripe of the dielectric material. An evanescent-wave mirror for the atoms is created by total internal reflection of a blue-detuned laser beam entering the film-vacuum interface. Indium tin oxide has a refractive index of $n \approx 2$, and a suitable dielectric material would be noncrystalline silicon nitride, which has $n = 2$ for $\lambda > 0.5 \mu\text{m}$ [17]. Given that the film thickness is constant, we can consider the film to be flat and homogeneous to the laser beam. If the beam is p-polarized and incident on the film-vacuum interface at an angle of 31° , which slightly exceeds the critical angle, the film-glass interface will impose only an insignificant loss to the light transmission ($\sim 0.4\%$), since the angle of incidence is close to the Brewster's angle. On the other hand, the evanescent-wave intensity on the upper surface of the film will be much higher than the beam intensity inside the film [18].

^a e-mail: andrej@focus.hut.fi

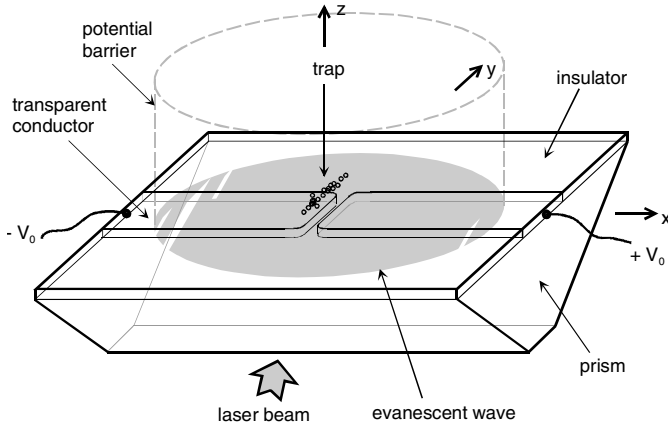


Fig. 1. Schematic diagram for realizing the electro-optical trap on an evanescent-wave mirror.

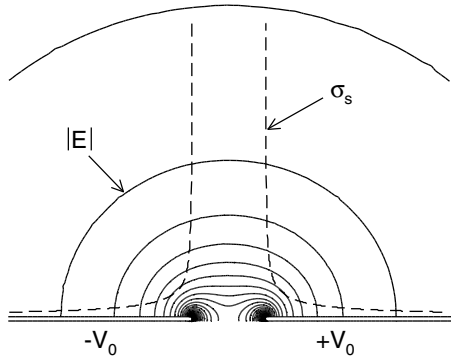


Fig. 2. Equipotential contours of the electric-field strength $|E|$ separated by $\Delta|E| \approx V_0 \times 6.5 \times 10^4$ V/m (solid line) and the absolute value of the surface charge density σ_s (dashed lines). The electrodes are separated by $2 \mu\text{m}$ and have a thickness of 100 nm .

The intensity decay length Λ of the evanescent wave will in this case be about 0.32λ .

When applying electrostatic potentials of $+V_0$ and $-V_0$ to the two ITO strips, the static electric field will be strong at the strip edges facing the gap. In Figure 2, equipotential contours of the electric-field strength within the vertical plane containing the symmetry axes of the strips are plotted as solid lines. The field is calculated by solving the 2D electrostatic Laplace equation assuming the thickness of the strips to be 100 nm and the width to by far exceed the strip separation which is taken to be $2 \mu\text{m}$. The dashed lines in the figure show the absolute value of the calculated surface charge density, σ_s , which quickly decays with the distance from the strip ends.

The potential of interaction between an atom and the static electric field and the evanescent wave is given by

$$U = -\frac{\alpha}{2k_B}|E|^2 + \frac{\lambda^3}{8\pi^2 ck_B} \frac{\Gamma}{\delta} I_0 \exp(-z/\Lambda), \quad (1)$$

where U is expressed in the equivalent temperature units. The parameter α denotes the electric polarizability of the atom, k_B is the Boltzmann's constant, c the velocity of light, Γ the natural width of the atomic line, and δ the de-

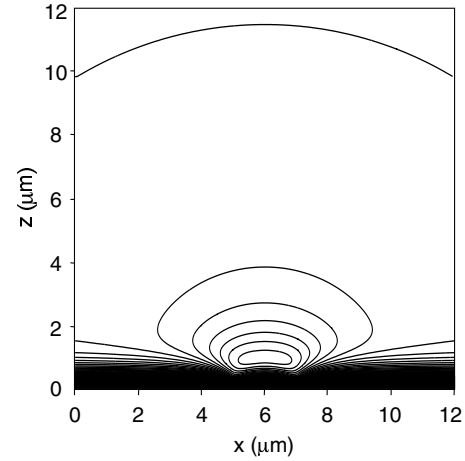


Fig. 3. Equipotential contours of the overall interaction potential. The step size is $\sim 2 \mu\text{K}$.

tuning of the evanescent-wave frequency from the atomic resonance with respect to the lower hyperfine ground state $|g1\rangle$ of the atom (for ^{133}Cs , this state is $|6^2S_{1/2}, F=3\rangle$). The quantity I_0 is the maximum value of the evanescent-wave intensity and z is the height above the film surface. Equation (1) has been written for an atom in the state $|g1\rangle$ in the limit of low saturation in the evanescent wave, neglecting both gravity and the van der Waals interaction, because their contributions to the trapping potential are insignificant (for ^{133}Cs , for example, the energy shift due to gravity is $< 1 \mu\text{K}$ at $z = 10 \mu\text{m}$; the evanescent-wave intensity is chosen to prevent the van der Waals attraction so that the potential barrier between the potential minimum and the surface remains much higher than the atomic thermal energy). Further calculations are done for the particular case of ^{133}Cs , for which the parameters are $\alpha = 6.6 \times 10^{-39} \text{ Cm}^2/\text{V}$, D_2 resonance wavelength $\lambda = 852 \text{ nm}$, and $\Gamma = 2\pi \times 5.3 \text{ MHz}$. The evanescent-wave intensity I_0 can reach values on the order of $1 \times 10^8 \text{ W/m}^2$ if the wave is excited by a p-polarized laser beam of 2.5 W with a beam diameter of $\sim 0.6 \text{ mm}$. Such a high value for I_0 allows δ to be large. If δ is equal to $2\pi \times 6200 \text{ GHz}$, which corresponds to a wavelength detuning of $\Delta\lambda \approx -15 \text{ nm}$, the value for V_0 may be taken to be 0.62 V . The potential U in the plane of Figure 2 is shown in Figure 3 as equipotential contours with a constant step of $\sim 2 \mu\text{K}$. The vertical and horizontal cross-sections of this profile, both containing the point of the potential minimum, are plotted in Figures 4a and 4b, respectively. This atom trap is $13.6 \mu\text{K}$ deep and has transverse dimensions on the order of a micrometer. The longitudinal size of the trap (in the y -direction) is determined by the width of the conductive strips.

Since the trapping field is created with transparent electrodes, the trap can readily be loaded with atoms from a gravito-optical surface trap (GOST), a trap produced by separating a part of the evanescent-wave atom mirror by a vertically aligned hollow laser beam [19–21]. Inside the GOST, the atoms are confined in the vertical direction by the evanescent wave and gravity, and in the horizontal

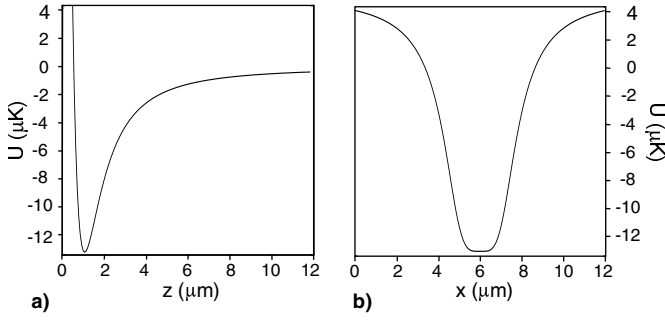


Fig. 4. Vertical (a) and horizontal (b) cross-section of the potential U of Figure 3.

directions by the surrounding potential barrier created by the hollow beam. The microtrap may be located in the middle of the GOST (see Fig. 1). Before turning on the voltage V_0 , the atoms in the GOST can be cooled to a temperature of a few μK through inelastic reflections from the evanescent wave [22]. At this step, the evanescent-wave detuning δ should be, for ^{133}Cs , on the order of $2\pi \times 1 \text{ GHz}$. The possibility to reach a temperature of $\sim 1 \mu\text{K}$ for Cs-atoms in a GOST has been predicted theoretically [22], and a temperature of $2 \mu\text{K}$ has been achieved in experiments [20]. When the atoms have been cooled down, the detuning δ may be increased to the value of $2\pi \times 6200 \text{ GHz}$ mentioned above. The voltage V_0 is then turned on. This will create a microscopic subtrap within the large gravito-optical trap. Part of the atoms is transferred into the subtrap, and the loading process is complete. If the GOST initially contains, e.g., 2×10^6 atoms, the thermalization time τ_{th} after the creation of the subtrap will be $\sim 0.5 \text{ s}$ [6].

A great advantage of this loading technique is the possibility to obtain a dense atomic sample in a tight microtrap from a large surface-mounted reservoir of cold atoms. Being dependent on the number of atoms transferred into the subtrap, the increase of the atomic temperature in the loading process can in fact be very small. Denoting the total number of the atoms by N_t , their initial temperature by T_i , the effective GOST volume by Ω_{GOST} , and the subtrap volume by Ω_{st} , we can assess the number of atoms transferred into the subtrap, N_{st} , as well as the final temperature T_f , by solving the coupled equations

$$T_f = T_i + \frac{2}{3} \Delta U_{st} \left(\frac{N_{st}}{N_t} - \frac{\Omega_{st}}{\Omega_{GOST}} \right), \quad (2)$$

$$\frac{N_t - N_{st}}{\Omega_{GOST} - \Omega_{st}} = \frac{N_{st}}{\Omega_{st}} \exp\left(-\frac{\Delta U_{st}}{T_f}\right), \quad (3)$$

where ΔU_{st} is the subtrap depth in units of temperature. The above equations are obtained by applying energy conservation and assuming a Maxwell-Boltzmann density distribution for the atoms. If, for example, the volume Ω_{GOST} is equal to $6.4 \times 10^{-12} \text{ m}^3$ (corresponding to a GOST diameter of 0.8 mm and a temperature T_i of $2 \mu\text{K}$) and the subtrap volume is $\Omega_{st} = 5 \times 10^{-16} \text{ m}^3$ (which is the case if the width of the conductive strips is $\sim 100 \mu\text{m}$), then, for $N_t = 2 \times 10^6$, we calculate the number of atoms in the subtrap to be $N_{st} \approx 6 \times 10^4$ and the temperature to be

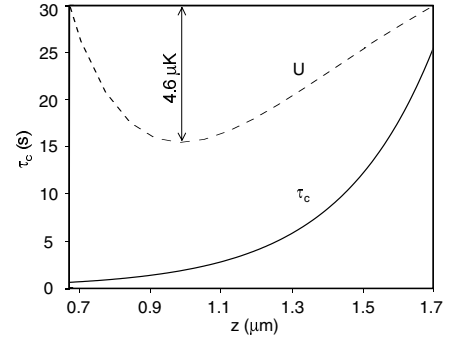


Fig. 5. The time τ_c (solid line) as a function of the vertical coordinate z across the trap center. The dashed line presents a fragment of the curve for U in Figure 4a. At $T_f = 2.3 \mu\text{K}$, the density of the atoms at the boundaries of the plot is $1/e^2$ times that in the trap center.

$T_f \approx 2.3 \mu\text{K}$. The local density of atoms in the microtrap will therefore be $n_0 \approx 1 \times 10^{20} \text{ m}^{-3}$. If the atomic sample is spin-polarized in advance, the local phase-space density will be $\Phi_{st} = n_0 \left(\hbar \sqrt{2\pi/mk_B T} \right)^3 \approx 0.1$ with m denoting the atomic mass. Such a high phase-space density is difficult, if not impossible, to reach in conventional (magnetic) microtraps without applying additional cooling by evaporation. The local enhancement of the phase-space density due to the mechanism described above has been demonstrated in an optical dimple trap created within a GOST [6]. This dimple trap is a microscopic dipole trap created by a vertical laser beam that is red-detuned far from the atomic resonance. The vertical size of the trap is mostly determined by the potential of gravity, while the horizontal size depends on the beam waist [6, 7]. For comparison, our trap can be designed to tightly confine atoms in all three directions or to serve as an atom guide that can be used in atom interferometry or in obtaining quasi-1D atomic gases.

Examining the loss mechanisms of the electro-optical trap, we first calculate the rate of optical transitions of the atoms in the evanescent wave. In the limit of a small saturation parameter S , the probability that an atom at rest at height z above the surface makes a transition from the state $|g1\rangle$ is given as a function of time t by $p = 1 - \exp(-\Gamma S t/3)$ [22]. Defining the characteristic time for the process by $\tau_c = 3/\Gamma S$ and expressing S in terms of the evanescent-wave intensity, we obtain

$$\tau_c = \frac{8\pi^2 \hbar c}{\lambda^3} \left(\frac{\delta}{\Gamma} \right)^2 \frac{1}{I_0} \exp(z/\Lambda). \quad (4)$$

The dependence of τ_c on z near the bottom of the trap is plotted as a solid line in Figure 5. The time τ_c at the minimum of the confining potential is equal to 2 s . Within this time the optical transitions can cause heating of the trapped atoms by $\Delta T \approx 2E_r/3k_B$, where E_r is the recoil energy. However, since the time τ_c is 4 times longer than the thermalization time τ_{th} and ΔT is equal to only 66 nK , the temperature in the microtrap will be essentially unaffected. On the other hand, while undergoing

optical transitions, an atom can get into the upper hyperfine ground state $|g2\rangle$ ($|6^2S_{1/2}, F = 4\rangle$) and then participate in a state-changing collision with another atom in the state $|g1\rangle$. As a result, both atoms will escape from the trap [19,22]. For ^{133}Cs , the mean branching ratio q_{12} to the state $|g2\rangle$ for transitions starting from $|g1\rangle$ is equal to 0.25. Taking into account the fact that in the end of the loading sequence, the collision time in the trap center is very short, we can conclude that the light-induced loss rate will be on the order of $\gamma_2 = 2q_{12}\tau_c^{-1} \approx 0.25 \text{ s}^{-1}$. Another loss mechanism in the subtrap is the three-body recombination. The coefficient K_3 for the recombination loss rate of Cs is not exactly known. However, if we assume $K_3 = 5.9 \times 10^{-28} \text{ cm}^6/\text{s}$, as is evaluated in [6], we calculate the loss rate γ_3 in the end of the loading to be $K_3\langle n^2 \rangle \approx K_3 n_0^2 / 3\sqrt{3} \approx 1.1 \text{ s}^{-1}$, where we have assumed that the trap is harmonic in all three directions. This maximum loss rate is nevertheless two times lower than the thermalization rate $1/\tau_{th}$ of the whole atomic sample in the GOST. Hence, the loss mechanisms will not significantly affect the loading efficiency, since the lost atoms will be immediately substituted with atoms from the GOST reservoir.

The high phase-space density that can be achieved in the proposed trap may allow a fast formation of a Bose-Einstein condensate by evaporative cooling. If the potential barrier created for the GOST by the hollow laser beam is removed, the atom reservoir is emptied, automatically leading to evaporation of atoms from the subtrap. The subtrap depth may be tuned by tuning either the voltage V_0 or the evanescent-wave intensity. Also, the detuning δ of the evanescent-wave frequency may be altered in order to increase the time τ_c . This provides an additional way to tune the trap depth.

Since the trap is non-magnetic, the confined atoms may be unpolarized or polarized into any particular magnetic substate. Choosing, for example, the lowest-energy magnetic state, which is the true ground state of the atoms, one obtains an atomic sample that is most stable against inelastic two-body collisions, which in this case have an endothermic character. Because of the low temperature in the trap, it becomes possible to create a Zeeman splitting of the atomic ground state that is much larger than the thermal atomic energy. Another consequence of the non-magnetic nature of the trap is the possibility to magnetically tune the interactions between the atoms without affecting the confining potential. Depending on the longitudinal size of the trap, it can serve as a tool for obtaining either a 3D or a quasi-1D degenerate quantum gas with a large fraction of the atoms being in the ground state of the trap.

In conclusion, we have described the basic principles of a microscopic electro-optical atom trap and analyzed the main trap characteristics for a simple trap geometry.

As the trap is based on non-magnetic confinement, it opens up a whole new level of flexibility for the design of microfabricated atom-optical devices.

We acknowledge financial support from the Academy of Finland and thank Prof. J. Javanainen for insightful comments.

References

1. W. Hänsel, P. Hommelhoff, T.W. Hänsch, J. Reichel, *Nature* **413**, 498 (2001)
2. H. Ott, J. Fortagh, G. Schlotterbeck, A. Grossmann, C. Zimmermann, *Phys. Rev. Lett.* **87**, 230401 (2001)
3. G. Birkl, F.B.J. Buchkremer, R. Dumke, W. Ertmer, *Opt. Commun.* **191**, 67 (2001)
4. R.J.C. Spreeuw, D. Voigt, B.T. Wolschrijn, H.B. van Linden den Heuvell, *Phys. Rev. A* **61**, 053604 (2000)
5. H. Gauck, M. Hartl, D. Schneble, H. Schnitzler, T. Pfau, J. Mlynek, *Phys. Rev. Lett.* **81**, 5298 (1998)
6. M. Hammes, D. Rychtarik, H.-C. Nägel, R. Grimm, *Phys. Rev. A* **66** 051401 (2002)
7. D. Rychtarik, B. Engeser, H.-C. Nägel, R. Grimm, [cond-mat/0309536](#)
8. M. Hammes, D. Rychtarik, B. Engeser, H.-C. Nägel, R. Grimm, [physics/0208065](#)
9. S.K. Sekatskii, B. Riedo, G. Dietler, *Opt. Commun.* **195**, 197 (2001)
10. J. Schmiedmayer, *Eur. Phys. J. D* **4**, 57 (1998)
11. R. Dumke, M. Volk, T. Mütter, F.B.J. Buchkremer, G. Birkl, W. Ertmer, *Phys. Rev. Lett.* **89**, 097903 (2002)
12. P. Krüger, X. Luo, M.W. Klein, K. Brugger, A. Haase, S. Wildermuth, S. Groth, I. Bar-Joseph, R. Folman, J. Schmiedmayer, [quant-ph/0306111](#)
13. R. Folman, P. Krüger, J. Schmiedmayer, J. Denschlag, C. Henkel, *Adv. At. Mol. Opt. Phys.* **48**, 263 (2002)
14. C. Henkel, P. Krüger, R. Folman, J. Schmiedmayer, [quant-ph/0208165](#)
15. D. Guéry-Odelin, J. Söding, P. Desbiolles, J. Dalibard, *Europhys. Lett.* **44**, 25 (1998)
16. A.J. Kerman, C. Chin, V. Vuletić, S. Chu, P.J. Leo, C.J. Williams, P.S. Julienne, *C.R. Acad. Sci. Paris IV* **2**, 633 (2001)
17. E.D. Palik, *Handbook of Optical Constants of Solids* (Academic Press, New York, 1998)
18. F. de Fornel, *Evanescent Waves From Newtonian Optics to Atomic Optics* (Springer-Verlag, Berlin, 2000)
19. Yu.B. Ovchinnikov, I. Manek, R. Grimm, *Phys. Rev. Lett.* **79** 2225 (1997)
20. M. Hammes, D. Rychtarik, V. Druzhinina, U. Moslener, I. Manek-Hönninger, R. Grimm, *J. Mod. Opt.* **47**, 2755 (2000).
21. I. Manek, Yu.B. Ovchinnikov, R. Grimm, *Opt. Commun.* **147**, 67 (1998)
22. J. Söding, R. Grimm, Yu.B. Ovchinnikov, *Opt. Commun.* **119**, 652 (1995)